RYERSON UNIVERSITY

FACULTY OF ENGINEERING, ARCHITECTURE AND SCIENCE

DEPARTMENT OF AEROSPACE ENGINEERING

Method for predicting damage sustained by air-backed plates subjected to impulsive loading from supersonic torpedo shock wave

Nicholas Mejia

AER870 Aerospace Engineering Thesis – Final Report

Faculty Advisor: Dr. Jeffrey Yokota

Date: April 2020

Abstract

A method is presented to estimate the severity of damage on an air-backed plate caused by the shock wave of a passing supersonic underwater torpedo. Theory of compressible liquid flows is used to calculate the pre- to post-shock density ratio and peak shock pressure of the torpedo. A Newtonian impact theory approach is then employed to obtain the shock standoff distance to the torpedo. Utilizing the density ratio, peak shock pressure, and standoff distance, a novel method for predicting the damage sustained by the plate from the shock wave is presented by equating the peak shock pressure and standoff of a torpedo to that of an underwater detonation of TNT. Well known theory for the effects of shock waves generated by TNT detonation is then used to determine the shock factor, damage number, and deflection-thickness ratio. Using these parameters, a sample design change to a steel plate is provided to reduce the shock factor to a negligible value for a case of Mach 1.4 torpedo at 7.5 body radii distance. The herein-presented process offers insight into how to improve naval ship hull design to prevent lethal damage from shock effects.

Acknowledgements

The author would like to acknowledge Dr. Jeffrey Yokota for agreeing to supervise this project. The time and advice he offered were crucial into the completion of the research. Particularly when challenges arose in building the problem and methodology, Dr. Yokota's advice was inspiring and helpful.

The author would also like to acknowledge Dr. Goetz Bramesfeld for his encouragement and advice over the duration of the project. Dr. Bramesfeld helped work through thought processes by lending an open ear countless times.

The author would also like to acknowledge Devin Barcelos, Travis Krebs, and all other friends in the Ryerson Applied Aerodynamics Laboratory of Flight who helped and listened to ideas along the way. Their support and friendship are greatly appreciated.

Contents

List of Figures

List of Tables

Nomenclature

a_0	freestream speed of sound
a_1	immediate after-shock speed of sound
C_p	pressure coefficient
I	Impulse
M	Mach number
P_0	freestream pressure
P_1	immediate after-shock pressure
P_s	surface static pressure
S	torpedo shock standoff distance
r	vehicle body radius
R	explosive shock standoff distance
W	weight of underwater explosive
W_e	weight of equivalent explosive

Greek letters

β	shock angle
β_s	sonic point angle measured from horizontal
$\left(\frac{\delta}{t}\right)_r$	deflection-thickness ratio for rectangular plate
η	coupling factor
θ	sonic point angle measured from vertical
ξ	shock factor
ξ_e	effective shock factor
ρ_0	freestream density
ρ_1	immediate after-shock density
τ	explosive time constant
ϕ_r	damage number for rectangular plate
ψ_a	dimensionless inverse mass number

1.0 Introduction

The structural response of materials to explosive blasts in water is of considerable importance to naval ship engineers for preventing loss of vessel and life. One of the first works in this field to theoretically describe underwater explosions and provide experimental data is by Cole who, in 1948, summarized most of the known, relevant hydrodynamic phenomena at the time [1]. This work laid the foundation for theory of supercavities in incompressible fluid which became a popular research area in the 50s and 60s relating to supercavitating torpedoes which have been designed to travel at velocities up to 500 km/h, a Mach of 0.10 in sea water near the surface. Supercavitating torpedoes are aptly named, as a cavity of water vapor encloses the torpedo structure. The cavity reduces overall drag on the vehicle by separating it from the water, allowing it to reach speeds on the order of five to ten times the speed of conventional underwater weapons [2]. In supercavitating flow, the cavitator contacts the freestream flow constantly and is responsible for inducing the vapor bubble. Supercavitating torpedoes induce this cavitation by using a blunted nose as a cavitator [3]. Petitpas et al. modelled cavitating flow around underwater missiles using a three-phase flow numerical method and show that at higher velocities, it is important to inject gas into the freestream from the cavitator to help induce cavitation [4].

As interest expanded to torpedoes moving at supersonic speeds in liquid, existing theory for supersonic gas flows was found to not provide accurate results for estimating the fluid behavior because of differences in the equations of state [5]. Notably, Nishiyama [5] applied the relations for a shock in air to calculate shock values in water. Vasin [6] shows that the results by Nishiyama do not agree with well-known theoretical and experimental results. Thus, the commonly used shock wave equations for relating pre- and post-shock parameters with Mach number are invalid in compressible liquid flows and a different approach is required to examine shock wave phenomena in liquids. In [1] a process is derived that allows the calculation of such parameters and [6] uses the described process across a range of Mach number. The process starts with choosing a peak shock pressure and relating it to freestream velocity,

Mach number, and the ratio of the pre- and post-shock densities. This process is detailed in the methodology section of the report.

Recently, countries like the USA and Russia have claimed to be developing torpedoes that exceed the speed of sound in water. Using the process in [1] and [5] shows that the pressures across the shock of a supersonic underwater torpedo (SUTOR) are enormous, exceeding 3000 MPa at Mach 2. Though these pressures can be calculated, the effect of a SUTOR shock wave on structures is not widely documented. Due to the massive energy requirements for thrust of the torpedo, the fact that SUTOR research is relatively new, and that any work done is likely behind military classification, there is little available data regarding capabilities or performance of such vehicles. It is possible that countries will build SUTORs in the future and it would be useful for designers of naval ships if there were a method to predict the effect a SUTOR's shockwave would have on a structure, namely, a ship's hull. While little research is available on the shock effects of a SUTOR, the shock effects of explosives is well documented and understood.

Several references discuss how to approximate the damage an underwater explosion's shock would have on a structure. For example, a semi-analytical method for elastic stresses and shock response of plates has been investigated and compared with experiments [7]. Ultimately, [7] proposed a strain energy distribution for the experimental data and found excellent agreement between the semi-analytical method and experimental data. Rajendran and Narasimhan conduct a review of the deformation and fracture behavior of plate specimens subjected to underwater explosions in [8]. The authors describe the sequence of events in an underwater explosion and discuss well known relations between the standoff distance of the shockwave emitted by an explosive charge, the peak pressure on that shock, and the charge weight, usually measured in kg of TNT. Additionally, they discuss various parameters such a shock factor, shock energy, and coupling factor. The shock factor is conventionally used to determine the severity of the effect of an underwater explosion on a sea vessel. Zhang and Jiang propose an improved shock factor for evaluation of small-sized structures [9]. In [9] the authors discuss the conventional shock factor and how it ignores the scattering effect of smaller structures, leading to overly severe shock

factors. Zhang and Jiang go on to propose an improved shock factor for small-sized structures by using a coupled mode method and decomposing the incident wave into a series of harmonic waves and conclude that it differs significantly from the conventional shock factor. Lee et al. investigate the deformation and rupture of thin steel plates from close-proximity underwater explosions [10]. The authors placed explosives at a desired standoff distance from steel plates and measured pressures at various locations and the displacement of the center of the steel plate. The experiment allowed data collection on the shock pressure, pressure history, gas bubble collapse, and plate deflection. The findings in [10] led the authors to conclude that deformation and failure of the plate could be dominated by the shock alone or by combination of both shock and bubble collapse, depending on the charge size, standoff distance, plate thickness, and plate properties. An underwater shock simulator was built to investigate the structural response to the shock of an underwater explosive for different material designs in [11]. Methods from [7] through [10] are used in this report and detailed in the methodology section.

This report presents a method to predict the structural response to an incoming shock wave generated by a passing SUTOR, something that is not currently well documented. That is, only the shock effects of the SUTOR are examined, not the effect of a detonation. The reason for this is that the peak pressures on a shock for a SUTOR are enormously large and the question of whether a SUTOR could inflict severe damage on a fleet of ships simply by travelling past was of interest. To do so, processes for calculating the peak shock pressure of a supersonic body in liquid flows are used from [1] and [6]. A method for calculating the shock standoff distance is then used from [12] and detailed in the methodology section. From [8] through [10], relations exist for the weight of an explosive and the peak pressure of a shock at a standoff distance after detonation. The shock peak pressure and standoff distance from processes in [1][6] and [12] are then used in the relation for explosive weight in [7] through [10] to find an equivalent explosive. That is, an explosive weight in kg of TNT is found to generate the same shock peak pressure at the same shock standoff distance as the shock generated by a body in a supersonic liquid flow. Then, using this equivalent weight, the effects on a structure can be determined using theory from

[7][8] and [10]. Predicting the damage a SUTOR can inflict by passing a ship will allow ship designers to understand lethal ranges for these future weapons and design hull thicknesses to alleviate the potential damage. A flow chart detailing this methodology and discussion is presented.

2.0 Methodology

Figure 1 shows a flowchart of the process that is used to proceed from calculating the shock characteristics to analyzing the effect of the shock on a structure.

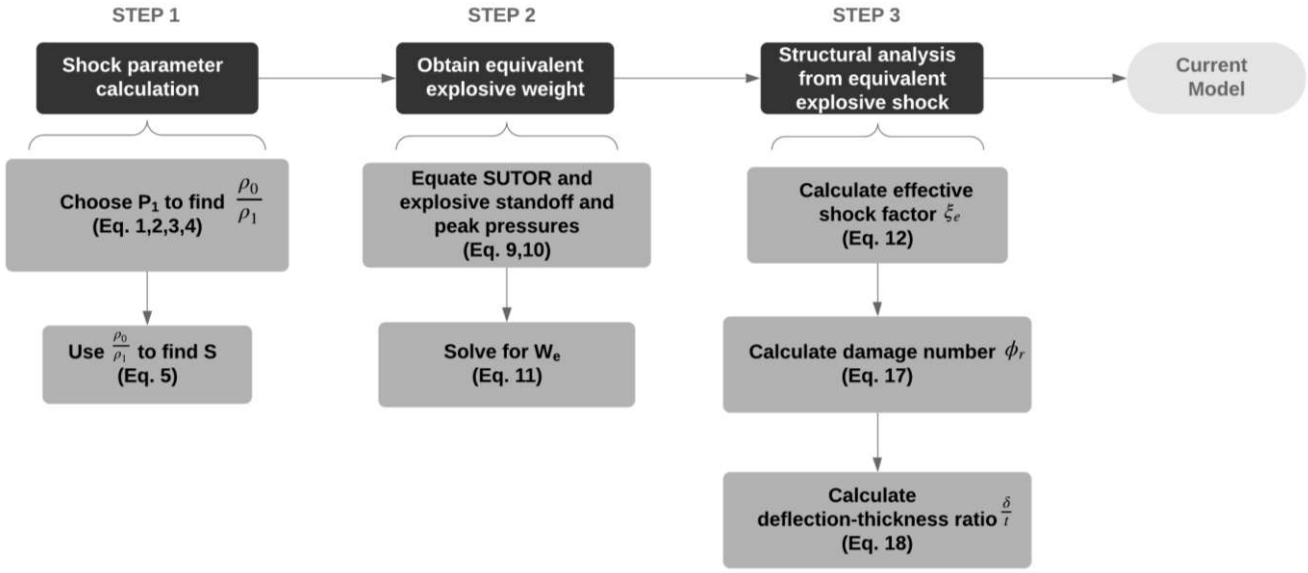

Figure 1: Flowchart outlining methodology

The process has three main steps: (1) shock parameter calculation, (2) obtaining the equivalent explosive weight, and (3) structural analysis from the equivalent explosive shock.

In step (1) the process outlined in [1] and [6] will be employed to generate the cross-shock density ratio in order to find the standoff distance of the shock from the SUTOR. As part of this process a means of estimating the shock standoff distance for a supersonic body in air is used [12]. In [12], Sinclair and Cui use a Newtonian impact theory approach to modify an experimental result for relating the shock

standoff distance for hypersonic flows around sphere to the freestream to after-normal-shock-density ratio along the central stagnation streamline. Their results include a relation for supersonic flows around circular cylinders and two relations based on one of two assumptions: (1) a linear density profile or (2) a linear Mach number profile between the shock wave and the body. This first step in this report will conclude with obtaining the shock standoff distance and peak pressures of the shock at any standoff for a SUTOR over a range of Mach numbers.

In step (2) the requirements for equating the shock generated by a SUTOR to the shock generated by an underwater explosive will be defined. To do so, the methods used in [7] through [10] are used to calculate the peak pressure at standoff from an underwater explosive, which is then related to an explosive weight in kg of TNT. The peak pressures and shock standoffs of the SUTOR in step (1) will then be used to find the equivalent weight in TNT to produce the peak pressure at standoffs from [7] through [10]. This step concludes with obtaining the equivalent weight in kg of TNT to generate the same peak pressure and standoff as the SUTOR at any specific Mach number as well as the decay constant for that shock pressure as it travels away from its initial location.

In step (3) the equivalent weight in kg of TNT and decay constant will be used to estimate the effect severity of the incoming shock from a SUTOR at various Mach numbers. The shock factor is calculated based on the equivalent weight in kg of TNT. The shock factor gives insight into the effect the incoming shock will have when it impacts the ship. The damage number is used to find the deflection-thickness ratio via an empirically derived equation for rectangular plates discussed [8][13]. The deflection-thickness ratio is the maximum deflection at the center of the impulse loaded plate. Step (3) concludes with obtaining the shock factor, damage number, and deflection-thickness ratio experienced by a rectangular plate that has been subjected to the shock wave generated by the equivalent weight of TNT at a range of standoffs.

2.1 Underwater shock parameter calculation

The shock angle and other relevant symbols are defined in Figure 2.

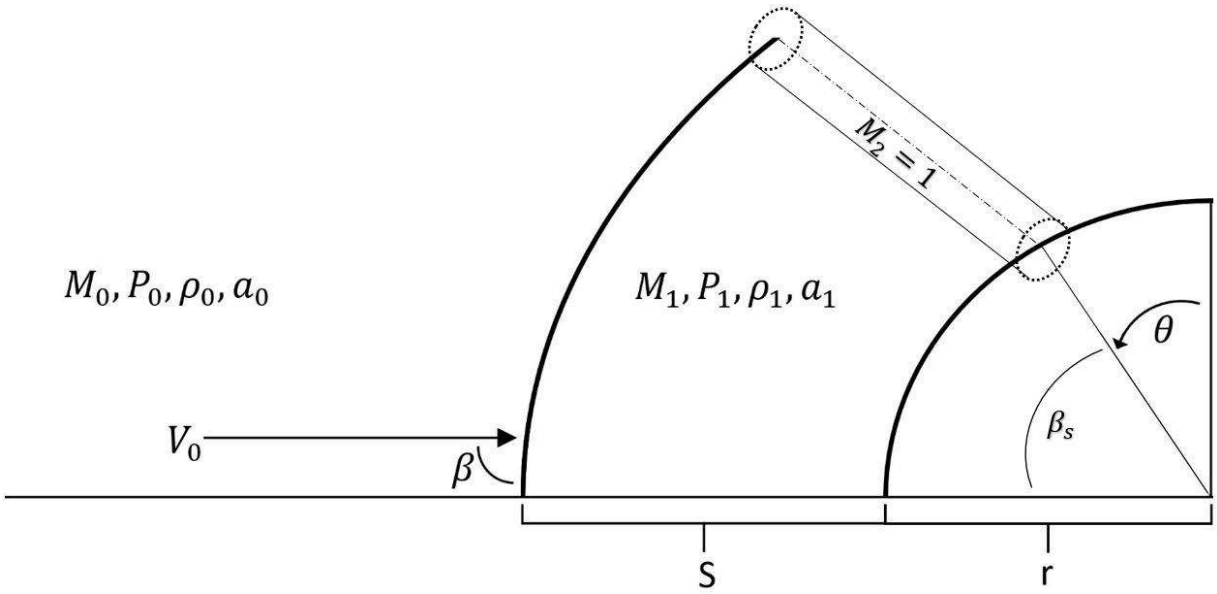

Figure 2: Shock and body diagram

The after-shock values of $M_1, P_1, \rho_1,$ and a_1 are defined to be the immediate after-shock values of Mach number, pressure, density, and speed of sound along a streamline that makes shock angle β with the freestream velocity, V_0. Here, a normal shock is defined to be $\beta = 90°$. The sonic point, where there exists a sonic stream tube with Mach number $M_2 = 1$ extending from the body to the shock is at an angle β_s from the central streamline or θ from the vertical axis. The shock standoff distance, S, is the distance from the body to the shock, and r, is the body nose radius. This report approximates the blunted nose of a SUTOR with a spherical nose.

The method presented in this report uses a well-known shock and static adiabatic curve relations expressed by the Tait equation [1] in the form:

$$P_1 - P_0 = B\left[\left(\frac{\rho_1}{\rho_0}\right)^n - 1\right] \quad (1)$$

The values B and n depend on the after-shock pressure, P_1, and for after-shock pressures less than 3000 MPa, the equation takes the form [6]:

$$P_1 - P_0 = B\left[\left(\frac{\rho_1}{\rho_0}\right)^n - 1\right], \qquad B = \frac{\rho_0 a_0^2}{n}, \qquad n = 7.15 \tag{2a}$$

and for after-shock pressures greater than 3000 MPa [4]:

$$P_1 - P_0 = d\left[\left(\frac{\rho_1}{\rho_0}\right)^k - 1\right], \qquad d = 416MPa, \quad k = 6.29 \tag{2b}$$

Behind the shock, the speed of sound can be determined from [1][6]:

$$a_1^2 = a_0^2\left(\frac{\rho_1}{\rho_0}\right)^{n-1} \tag{3}$$

The dependency of the density ratio, $\frac{\rho_1}{\rho_0}$, freestream Mach number, M_0, and shock angle, β, is, for after-shock pressures less than 3000 MPa [6]:

$$M_0^2 sin^2\beta = \left[\left(\frac{\rho_1}{\rho_0}\right)^n - 1\right]\left[n\left(1 - \frac{\rho_1}{\rho_0}\right)\right]^{-1} \tag{4a}$$

and for after-shock pressures greater than 3000 MPa [6]:

$$M_0^2 sin^2\beta = \left[\left(\frac{\rho_1}{\rho_0}\right)^k - 1\right]\frac{d}{\rho_0 a_0^2}\left(1 - \frac{\rho_0}{\rho_1}\right)^{-1} \tag{4b}$$

To calculate the flow characteristics behind the shock, first, an after-shock pressure, P_1, is chosen. From this, the ratio of densities is found with equation (2) and the speed of sound with equation (3). The Mach number at a specific shock angle is then found using equation (4). It should be noted that since the freestream pressure, P_0, is orders of magnitude smaller than any after-shock pressure, P_1, it can considered negligible [1]. This report only considers the pressures across a shock angle of 90°.

Once the shock parameters are known, the standoff distance, S, can be calculated using a modified Newtonian impact theory approach by Sinclair and Cui [12]. The conventional linear density profile

approach discussed in [12] is used as the authors concluded that it showed better agreement at Mach numbers lower than 5 and the maximum Mach number considered in this report is 3.184. Experimental measurements of shock standoff distances around spheres show that the ratio of standoff distance to sphere radius correlates with the ratio of the freestream density to the after-shock density by [12]:

$$\frac{S}{2r} = 0.41\frac{\rho_0}{\rho_1} \tag{5}$$

With the density ratio known from equation (2) and the vehicle radius, r, being a design parameter, the shock standoff distance, S, can be found.

The shock standoff distance can be plotted up to the sonic point following a method by Sinclair and Cui [12]. A proposed modification to the Newtonian impact theory discussed in the report for the sonic point is given by:

$$\frac{C_{p,s}}{C_{p,max}} = sin^2\theta \tag{6}$$

$$\beta_s = \frac{\pi}{2} - sin^{-1}\sqrt{\frac{C_{ps}}{C_{p,max}}} \tag{7}$$

Where $C_{p,s}$ is the pressure coefficient at the sonic point on the body and $C_{p,max}$ is the maximum pressure coefficient. The pressure coefficient calculations are derived in [12] and are:

$$C_{p,max} = \frac{2}{\gamma M_0^2}\left\{\left[\frac{(\gamma+1)^2 M_0^2}{4\gamma M_0^2 - 2(\gamma-1)}\right]^{\gamma/\gamma-1}\left[\frac{1-\gamma+2\gamma M_0^2}{\gamma+1}\right] - 1\right\} \tag{8}$$

$$C_{p,s} = \frac{2}{\gamma M_0^2}\left\{\left(\frac{\gamma+1}{2}\right)^{-\gamma/\gamma-1}\left[\frac{(\gamma+1)^2 M_0^2}{4\gamma M_0^2 - 2(\gamma-1)}\right]^{\gamma/\gamma-1}\left[\frac{1-\gamma+2\gamma M_0^2}{\gamma+1}\right] - 1\right\} \tag{9}$$

Utilizing the freestream Mach number calculated from equation (4) the angle from the central streamline to the sonic point on the blunt nose body can be calculated using equations (6) through (9). Since the body radius is a design parameter, the bow shock can be plotted from the central streamline up to the

sonic point. This result is not used in the analysis of the shock effect on a structure but is of interest if the pressures at different angles from the central streamline were to be investigated in the future.

2.2 Obtaining the equivalent explosive weight

Equating the vehicle shock characteristics calculated in section 3.1 to the shock of an underwater explosion is necessary to approximate the shock effects a SUTOR would have on a structure. Underwater explosive effects on surfaces is well documented and data is widely available on the topic. The relevant geometrical relations of an explosive are shown in Figure 3.

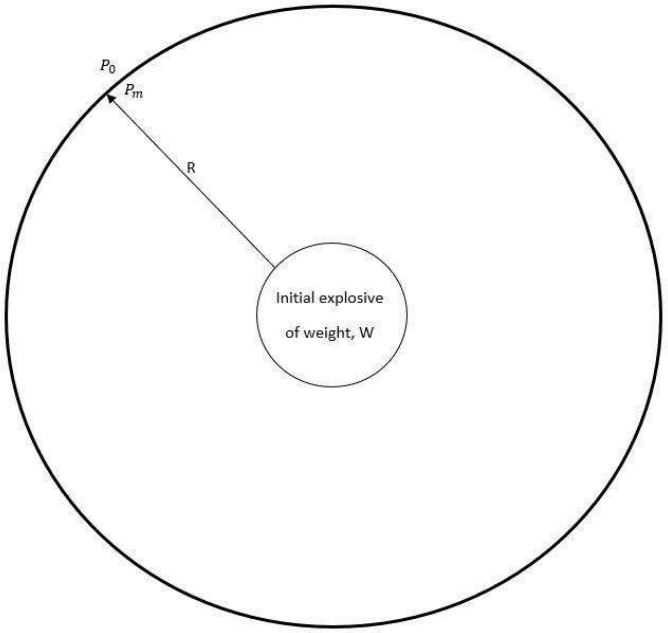

Figure 3: Explosive shock and standoff diagram

The diagram shows the relevant parameters for an explosive with equivalent weight in TNT, W, and the shock wave it would generate after detonation at a standoff, R in a fluid with undisturbed pressure P_0. The peak shock pressure, P_m, is defined as the pressure on the incident shock front at some standoff distance R. For all analysis relating to the explosive, it is assumed that all detonation reactants are consumed, and

the explosive geometrical size is negligible, a common practice in the referenced explosive research. Additionally, most explosives are compared to each other by their equivalent weights in TNT, so any relations will use values for TNT.

In general, the pressure time history, $p(t)$, starts with a near instantaneous increase to the peak pressure, P_m, as the shock front arrives, followed by a decay to the original hydrostatic pressure [8]. This decay at a fixed location is modeled by [8]:

$$p(t) = P_m e^{-t/\tau} \tag{10}$$

Where t is time from the initial detonation and τ is the decay constant. The peak pressure and decay constant depend on the size of the explosive charge and the distance from the charge to the point [8]:

$$P_m = K_1 \left(\frac{W^{1/3}}{R}\right)^{\alpha_1} \tag{11}$$

$$\tau = K_2 W^{1/3} \left(\frac{W^{1/3}}{R}\right)^{\alpha_2} \tag{12}$$

where K and α are shock parameters unique to the explosive. For TNT, these equations take the form:

$$P_m = 52.16 \left(\frac{W^{1/3}}{R}\right)^{1.13} \tag{13}$$

$$\tau = 96.5 W^{1/3} \left(\frac{W^{1/3}}{R}\right)^{-0.22} \tag{14}$$

From section 3.1, SUTOR shock standoff distance, S, and shock front pressure, P_1, are known. Using Equation (11), the weight of a TNT explosive to generate a shock with equal peak pressure at a standoff distance to the SUTOR, W_s, can be found under the following requirements:

$$P_m = P_1 \tag{15}$$

$$S = R \tag{16}$$

and is then given by using the requirements in equations (15) and (16) in equation (11):

$$W_e = \left[S \left(\frac{P_1}{52.16} \right)^{1/1.13} \right]^3 \tag{17}$$

With the equivalent explosive weight, W_e, known, the pressure-time history at distances away from the incident shock generated by a SUTOR can be estimated using equations (10), (11), and (12). With the pressure at any distance from the SUTOR calculable, the structural response to the shock can now be investigated.

2.3 Structural analysis on effects of the equivalent explosive shock

Predicting the structural response to an incoming shock generated by a supersonic underwater vehicle is important for future design of ships. A widely used indication of damage a sea vessel would sustain from the shock of an explosive is the shock factor given by [8][10]:

$$\xi = 0.445 \frac{\sqrt{W}}{R} \tag{18}$$

In general, for a shock factor under 0.15 the damage sustained is considered negligible, while for shock factors over 0.70, the damage is the severest, and likely lethal to the vessel [10][13]. Equation (18) can be used with the equivalent explosive weight, W_e, to find the shock factor experienced by a structure from a SUTOR and can be calculated for different distances between the SUTOR and target, R.

To analyze the deformation-thickness ratio of an air-backed plate, the dimensionless inverse mass number is introduced [8][13]:

$$\psi_a = \frac{\rho_w a_w \tau}{m} \tag{13}$$

where ρ_w and a_w is the density and speed of sound in water, respectively, τ is from equation (14), and m is the mass per unit area of the plate. Using this number, the coupling factor is found by [8][13]:

$$\eta = 4(\psi_a)^{1+\psi_a/1-\psi_a} \tag{14}$$

The effective shock factor considering scattering is then given by [9]:

$$\xi_e = \xi^{1.03}\sqrt{\eta} \tag{15}$$

The impulse per unit area of an air-backed plate in terms of effective shock factor is derived in [8][9] and is given by:

$$I_{pa} = 963\xi_e\sqrt{m} \tag{16}$$

The plastic damage on a plate undergoing an impulsive load can be described by a dimensionless number called the damage number, and for a rectangular plate is given by [8][13]:

$$\phi_r = \frac{I_t}{2t^2\sqrt{4ab\rho_p\sigma_y}} \tag{17}$$

where I_t is the total impulse, ρ_p and σ_y are the plate material densities and material yield stress, respectively, $2a$ and $2b$ are the lengths and breadths of the plate, and t is the thickness of the plate. The deflection-thickness ratio for rectangular plates is then given by [8][13]:

$$\left(\frac{\delta}{t}\right)_r = 0.553\phi_r + 0.741 \tag{18}$$

3.0 Sample application

The capability of the proposed procedure is presented in a test case of a SUTOR with a unit radius blunt nose. First, equations (1) through (4b) will be used to determine the flow parameters at various after-shock pressures. As mentioned in section 2.1, the peak pressure on the shock front is chosen first, and the related Mach number calculated from it.

The determined flow parameters V_0 and a_1 from section 2.1 are compared over a range of peak shock pressure, P_1, with the parameters found in [1], V' and a', and with [6], V'' and a'', in Table 1 with Mach numbers shown for reference.

Table 1: Comparison of shock related flow parameters to references

M	$P_1\ [MPa]$	$V_0\ [^m/_s]$	$V'\ [^m/_s]$	$V''\ [^m/_s]$	a_1	a'	a''
1.356	490	1939	1967	1975	2196	2221	2230
1.597	980	2284	2310	2335	2711	2734	2755
1.790	1470	2560	2586	2630	3121	3142	3175
1.956	1960	2797	2823	2880	3469	3491	3535
2.103	2450	3007	3033	3110	3776	3798	3855
2.236	2940	3198	3223	3320	4054	4075	4140
2.373	3430	3936	3394	3510	4241	4343	4405
2.482	3920	3549	3550	3690	4497	4605	4650
2.682	4900	3835	3836	4020	4969	5088	5100
2.863	5880	4094	4095	4325	5397	5527	5505
3.029	6860	4332	4333	4610	5793	5931	5880
3.184	7840	4553	4554	4885	6162	6309	6240

The calculated values by the author show close agreement across the peak pressure range in Table 1 with those calculated in [1] and [6].

The shock standoff distance from the SUTOR will be examined for a Mach 2.373 flow case. The determined flow parameters from equation (2) and (3) are used in equation (5) to find the shock standoff distance. Figure 4 shows a plot of the SUTOR blunt nose of unit radius and shock up to the sonic point angle, β_s.

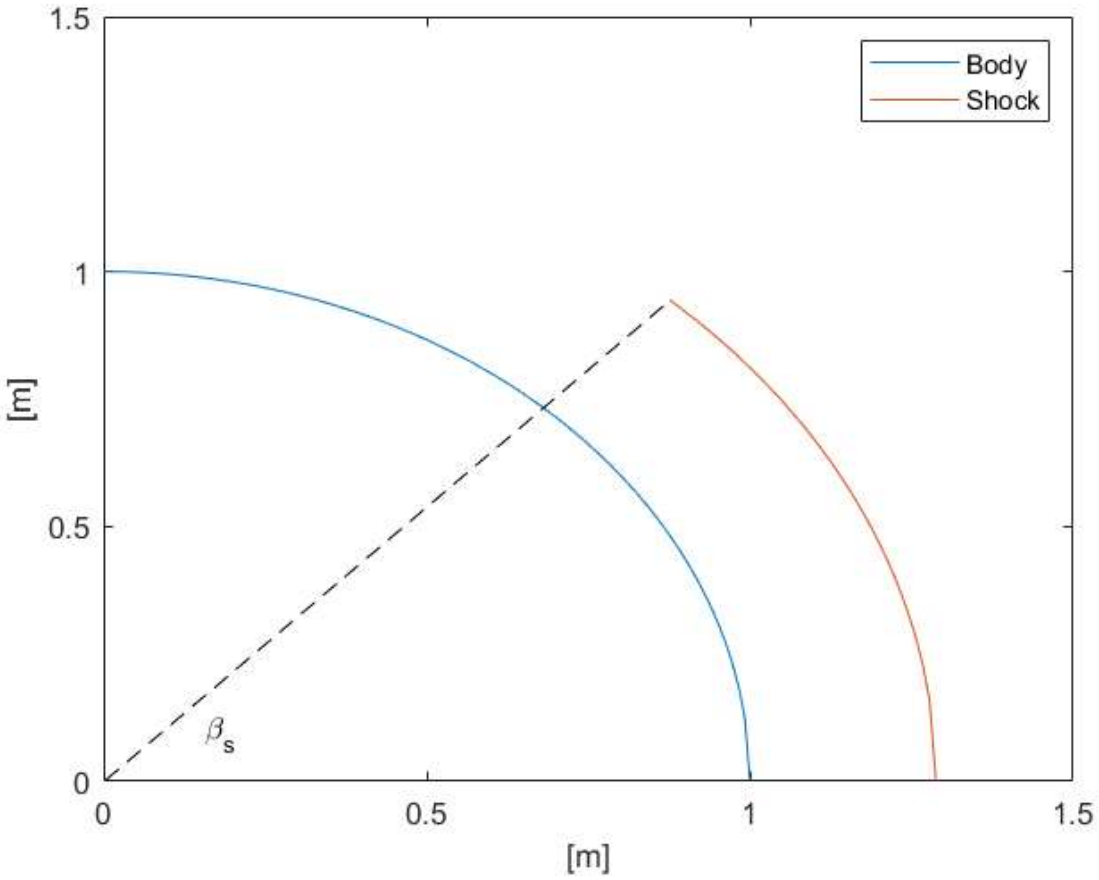

Figure 4: Standoff distance from Mach 2.373 sphere-head in liquid flow

The standoff distance was found to be 0.287 meters for a freestream Mach number of 2.373. With the standoff distance known, the equivalent explosive weight can be obtained for the Mach number of 2.373 from equation (17) using conditions (15) and (16) and is plotted versus experimental data from [1] over a range of body radii, or standoff, from 0.5 to 12.5 in Figure 5.

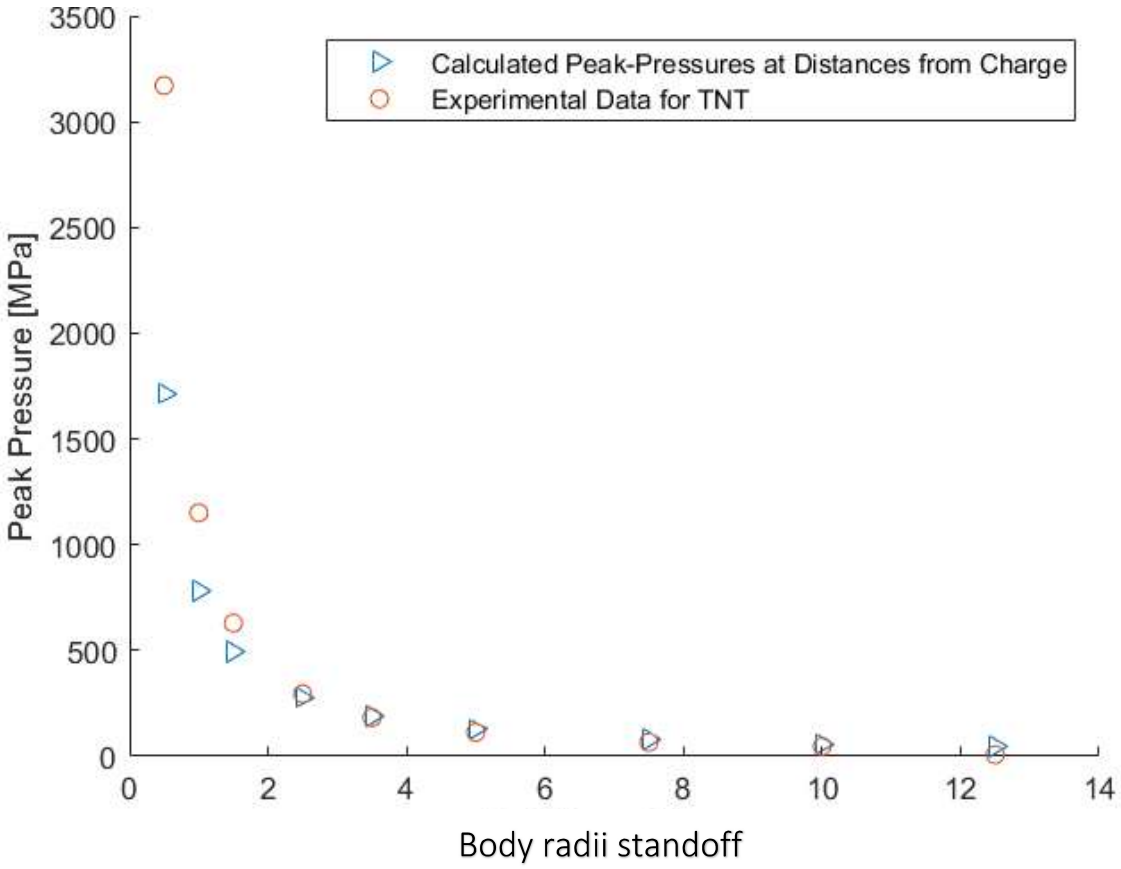

Figure 5: Comparison of experimental peak pressures and calculated peak pressures over a range of body radii standoff

The process in this report tends to underpredict the peak pressures close to the explosive but has good agreement past two body radii. Only the case of M=2.373 is shown because it is the only case with experimental data for comparison.

Following the procedure in 2.3, the shock factor, damage number, and deflection-thickness ratio can be found using the equivalent explosive weight. To do so, a square plate of unit area and thickness of $\frac{3}{8}$ inches is used for calculation. At Mach numbers from 1.4 to 3.1, the equivalent explosive weight is calculated and used to find the shock factors over an explosive radii range from 0.5 to 12.5 and is plotted in Figure 6.

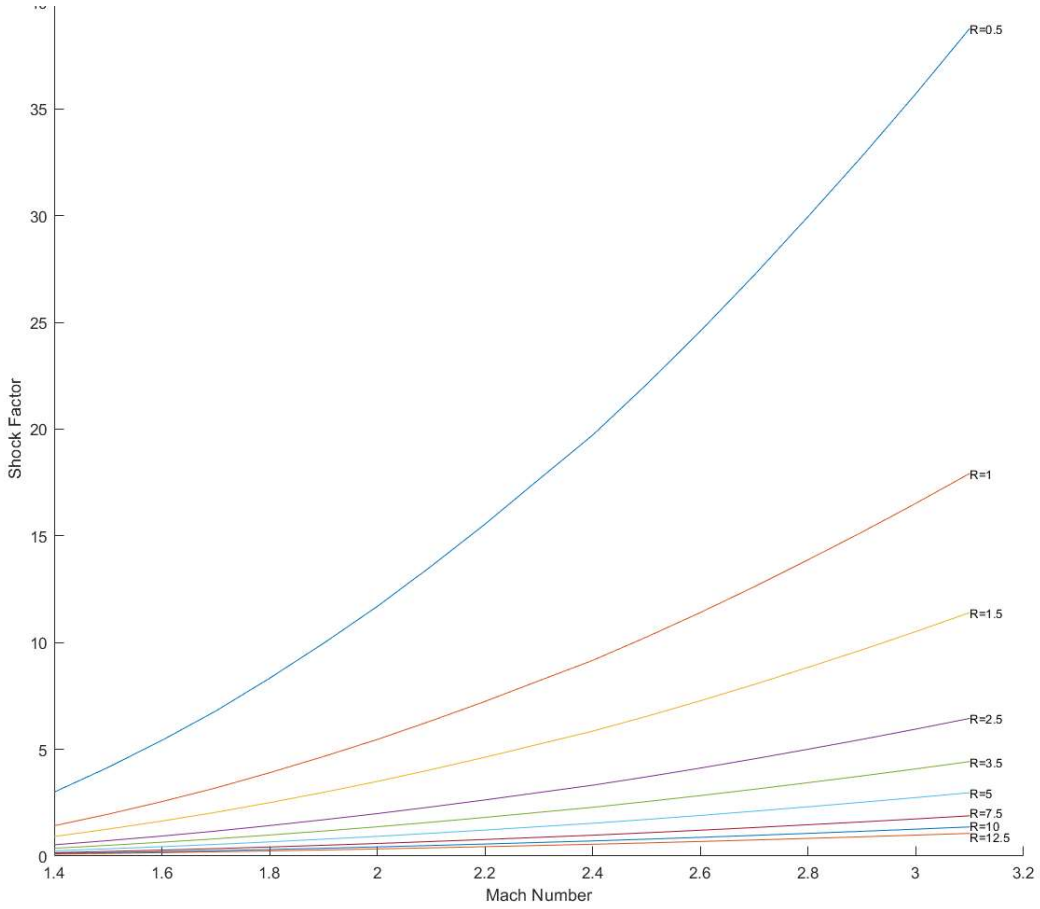

Figure 6: Shock factors experienced by a plate at various standoffs and Mach numbers

The figure shows that the shock factor is significant over most ranges of Mach number and standoff.

Figure 7 shows the same data while limiting the shock factor to below 0.7.

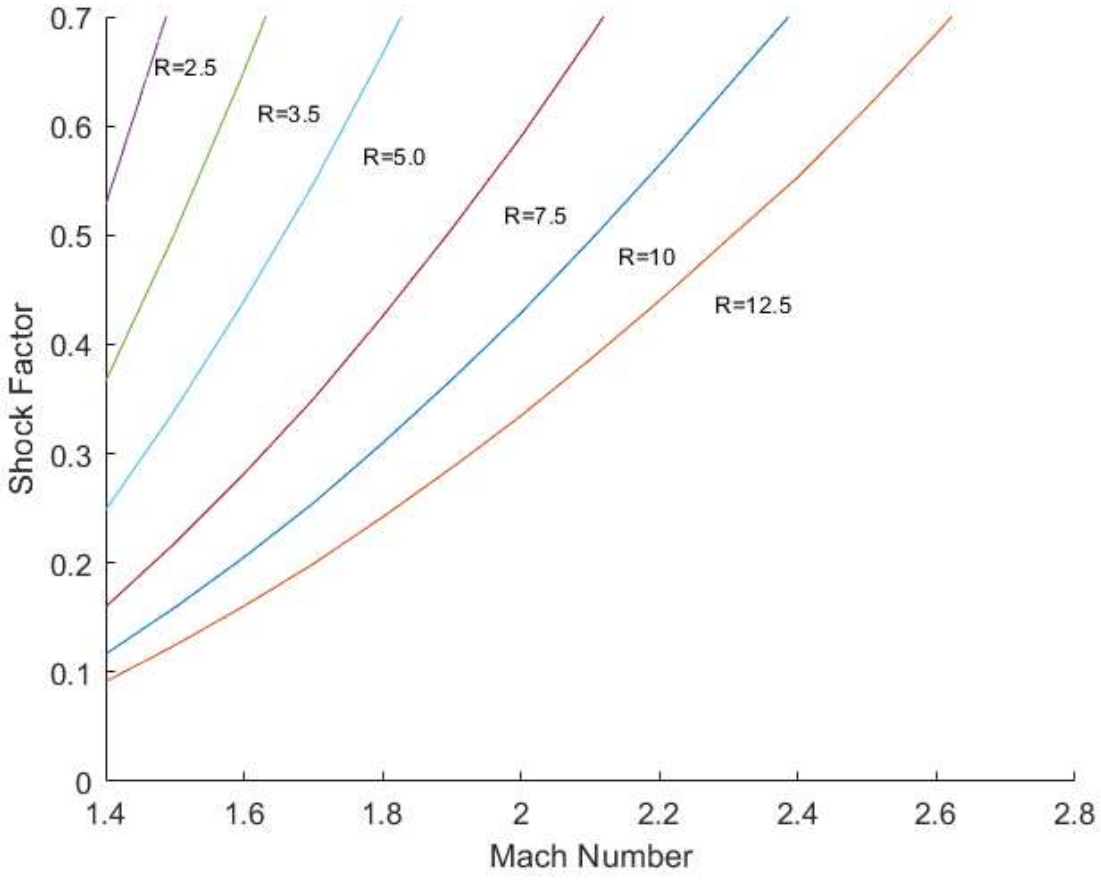

Figure 7: Shock factor limited to 0.7 experienced by a plate at various standoffs and Mach numbers

Figures 6 and 7 show that the air-backed plate would experience shock factors that exceed the negligible shock factor limit of 0.15 for most Mach numbers over the standoff ranges examined, and most of the shock factors would be classified as lethal.

From the shock factor, the deflection-thickness ratio can be calculated by equation (18). The deflection-thickness ratio is plotted against the shock factor in Figure 8 and against the damager number in Figure 9:

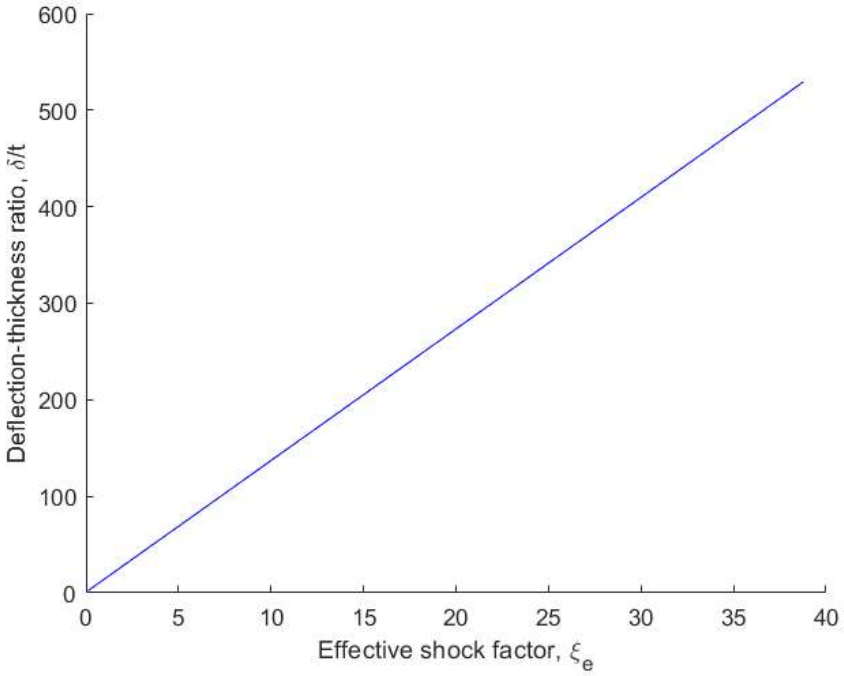

Figure 8: Deflection-thickness ratio of a plate at various effective shock factors

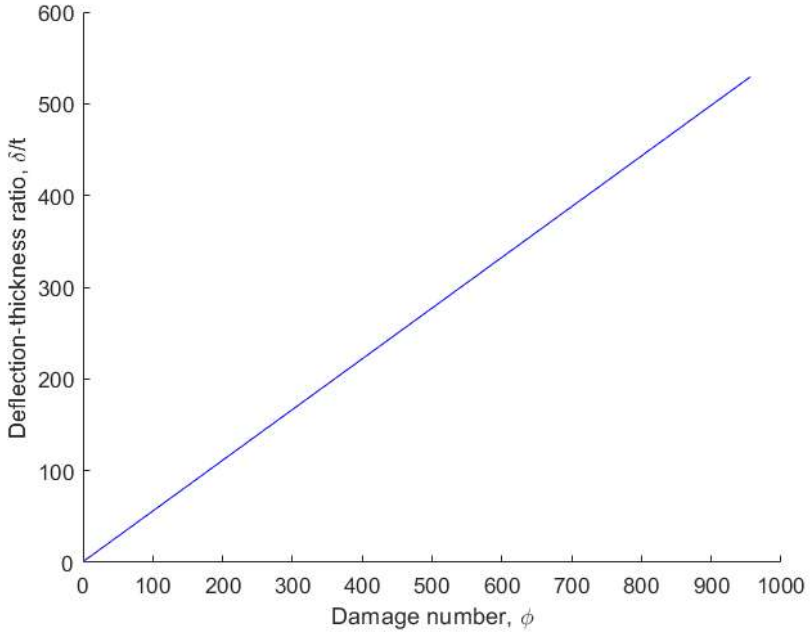

Figure 9: Deflection-thickness ratio of a plate at various damage numbers

The figures show large deflection-thickness ratios. This is because the theory used to model the deflection assumes that fracture has not occurred. From figure 6 and 7, only lower Mach number cases with larger

body radii ranges produce shock factors that do not cause uncontrollable flooding. Most Mach number, body radii combinations are well past this shock factor threshold of 0.7.

As an example of how the results can be used to improve the design of a plate that is close to the shock factor threshold of 0.15 for negligible damage, a design change is provided for the case of a Mach number 1.4 SUTOR passing at body radii range of 7.5. Table 2 shows the relevant values for the results from this report and the design requirements for an improved plate:

Table 2: Parameters of selected case and design requirements

Parameters	M	R	Shock Factor	ϕ_r	$\left(\frac{\delta}{t}\right)_r$	t [m]	a [m]	b [m]
Original plate	1.4	7.5	0.1595	3.9332	2.9161	0.009535	0.5	0.5
Improved Plate	1.4	7.5	0.1500	TBD	TBD	TBD	TBD	TBD

From figures 8 and 9, the damage number and shock factor are related through the deflection-thickness ratio. In order to reduce the shock factor to 0.1500, the related deflection-thickness ratio is found first. For a shock factor of 0.1500, the related deflection-thickness ratio from figure 8 is 2.045. At a deflection-thickness ratio of 2.045, the damage number is 3.697 from figure 9. The improved design damage number to original ratio is given by using equation (17):

$$\frac{\phi_{r,improved}}{\phi_{r,original}} = \frac{\frac{I_t}{2t_i^2\sqrt{4a_ib_i\rho_p\sigma_y}}}{\frac{I_t}{2t^2\sqrt{4ab\rho_p\sigma_y}}} \tag{19}$$

Assuming the material does not change, the only parameters that change are the dimensions of the plate. Using the shock factors in table 2 and the plate dimensions used in this report, equation (19) reduces to:

$$0.9404 = \frac{0.0048}{t_i^2\sqrt{a_ib_i}} \tag{20}$$

From (20), the geometric requirements to reduce the shock factor to 0.1500 is given. Since the intention is for the method to be used for ship's hulls, the length and breadth are likely not changeable, so the thickness is modified, and the updated parameters are shown in table 3:

Table 3: Final parameters for shock factor reduction

Parameters	M	R	Shock Factor	ϕ_r	$\left(\frac{\delta}{t}\right)_r$	t [m]	a	b
Original plate	1.4	7.5	0.1595	3.9332	2.9161	0.009535	0.5	0.5
Improved Plate	1.4	7.5	0.1500	3.697	2.015	0.009800	0.5	0.5

Increasing the plate thickness to 0.0098 meters reduces the shock factor to 0.15, the threshold for negligible damage.

4.0 Discussion of Results

In step (1) the standoff distance for a shock generated by a SUTOR is found. In Table 1 the results for calculating the flow parameters of a shock are displayed and compared with data from [1] and [6]. The calculated values match excellently and so there is high degree of confidence in this procedure. However, the method in [12] describes how to determine the shock standoff distance for a sphere in a supersonic gas flow. Since it is well known that the shock equations for a gas do not work in liquid from references [5] and [6], it is appropriate to assume that an empirically derived relation for shock standoff in gas is inaccurate for the standoff in liquid. Methods for determining shock standoff are generally done through computational fluid dynamics or empirical means. A CFD supersonic liquid flow solver was not available and building one would require time outside the scope of this report. Additionally, empirical relations for liquid shock standoffs are not well documented and no such relation could be found. Therefore, the relation by Sinclair and Cui in [12] is the only feasible way to predict the standoff and future experiments or work should focus on this step when attempting to verify whether the process in this report is sound.

In step (2) the equivalent explosive weight is found. That is, the weight of a TNT explosive required to generate a shock with a peak pressure and standoff that is equal to that of the SUTOR at a Mach number is found. This relation is then used to find the peak pressure of the incident shock as it travels from 0.5 to 12.5 body radii away from the SUTOR and is compared to experimental data from [1] for TNT. These results match well past two body radii even though the requirement for this analysis relied on the standoff method in [12]. This could suggest that the method in [12] is applicable for liquid flows under certain parameter.

In step (3) the shock factor, damage number, and deflection-thickness ratio are found for a shock wave generated by an equivalent weight explosive. The thin plate procedure used found lethal shock factors are most Mach numbers for a SUTOR at most standoffs, as seen in Figures 6 and 7. At larger body radii distances, the SUTOR still caused severe shock factors to be experienced as Mach number increased. The deflection-thickness ratio was then found and plotted versus the shock factor and damage numbers. The deflection-thickness ratios use linear elastic theory to determine the maximum deflection at the center of the impulse loaded plate. The results are too large to be useful, as the severity of the shock factors are far beyond what would cause uncontrollable flooding. This means the plates have already failed and deflection is not a useful measure of damage. In references [8] and [13] the deflection-thickness ratio maximum value was about 35 for a damage number of about 45. Looking to figure 9, it does appear that this deflection-thickness ratio would occur at that damage number. This is expected since equation (18) is linear and is empirically derived for air-backed plates. Thus, if the SUTOR does generate a shock as modelled in this report, there is confidence in the severity of damage predicted. An example case for reducing the shock factor to a negligible damage threshold is given.

While there is confidence in this method if the shock severity is correct, the method used was for thin, air-backed plates. The exact design of the hull and armor systems of naval ships is not known and likely much more complex. This section of part (3) would need to be re-examined for each combination of ship and hull armor design and would likely have to be done on a case by case basis. As such, the results likely

over predict damage since armor and hull design are not considered. Additionally, the method for determining the shock factor, damage number, and deflection-thickness ratio required plate dimensions. In this report a square plate of unit area and $\frac{3}{8}$ thickness is used to analyze the effect of the shock and the assumption of the entire plate being impulsively loaded is used. This means that the results are sensitive to these geometrical assumptions and experiments would need to be done on a range of dimensions to be applied to ship design.

To improve on this method in ways other than previously mentioned, a larger range of body radii should be examined in step (2). The maximum range of 12.5 body radii was chosen because that was the only data available for comparison. Whether it is realistic to assume a SUTOR could reach this proximity to a naval vessel before being intercepted is a topic for discussion when these weapons exist. If they can travel past a ship within 12.5 body radii, the ship will likely sustain severe to lethal damage, depending on Mach number. If not, then as the method should be extended to larger body radii distances and new experiments should be conducted to validate the method at these distances. Additionally, the deflection-thickness ratio was inadequate at relatively large damage numbers. The deflection-thickness ratio can only be used prior to onset of fracture or total failure. When the shock factor is less than 0.7, uncontrollable flooding has not occurred yet. This means that for any shock factor under 0.7, the deflection-thickness ratio can be used to design future ships while preparing for future underwater weapons technology capabilities.

While the deflection-thickness ratio mostly shows total failure of the plate, it does give insight into lethal cruise standoffs for these weapons. This means that when designing the defensive systems of next generation warships, engineers can look at the range and Mach number combinations that generate lethal shock factors and compare them to the relevant weapons technology progress. With an expectation of the capability of SUTOR technology during a newly designed ship's expected lifetime, the ship's defensive systems can be designed to be able to prevent a SUTOR from entering the lethal shock factor distance.

5.0 Conclusion

This report presents an approach to predict the damage an air-backed plate would sustain from a shockwave generated by a passing supersonic underwater torpedo. Equivalent weights in TNT are found to generate the same shock peak pressures at the same standoff distances as a SUTOR at various Mach numbers and body radii ranges. The equivalent weight in TNT is then used to find the shock factor, damage number, and deflection-thickness ratio for a fully loaded air-backed plate. A sample design change is provided to lower the shock factor to a negligible damage threshold by changing the plate geometry to lower the damage number.

The introduced approach has the potential to advance the development of naval ship hull systems for preventing severe damage from shock effects. Countries have already shown interest in designing SUTORs, but existing methods and theory for the shock damage they could induce are not well documented. Although the current report contains various methods that require experimental verification before being used for design, it provides insight into the importance that the shock effects be well understood for future hull design.

References

[1] Cole, R. H., *Underwater Explosions*, London, UK: Oxford University Press, 1948.

[2] Alyanak, E., Grandhi, R., and Penmetsa, R., "Optimum design of a supercavitating torpedo considering overall size, shape, and structural configuration," *International Journal of Solids and Structures*, Vol. 43, No. 3, 2006, pp 642-657.

[3] Choi, J. H., Penmetsa, R. C., and Grandhi, R. V., "Shape optimization of the cavitator for a supercavitating torpedo," *Structural and Multidisciplinary Optimization*, Vol. 29, No. 2, 2005, pp. 159-167.

[4] Petitpas, F., Saurel, R., Ahn, B., and Ko, S., "Modelling cavitating flow around underwater missiles," *International Journal of Naval Architecture and Ocean Engineering*, Vol. 3, No. 4, 2011, pp. 263-273.

[5] Nishiyama, T., and Khan, O. F., "Compressibility Effects on Cavitation in High Speed Liquid Flow (Second Report-Transonic and Supersonic Liquid Flows," *Transactions of the Japan Society of Mechanical Engineers Series B*, Vol. 47, No. 416, 1981, pp. 655-661.

[6] Vasin, A. D., "Supercavities in Compressible Fluid," *North Atlantic Treaty Organisation Research and Technology Organisation, Supercavitating Flows,* RTO-EN-010, pp. 16.1-16.29.

[7] Rajendran, R., and Narasimhan, K., "Linear elastic shock response of plane plates subjected to underwater explosion," *International Journal of Impact Engineering*, Vol. 25, No. 5, 2001, pp. 493-506.

[8] Rajendra, R., and Narasimhan, R., "Deformation and fracture behavior of plate specimens subjected to underwater explosion—a review," *International Journal of Impact Engineering*, Vol. 32, No. 12, pp. 1945-1963.

[9] Zhang, W., and Jiang,m W., "An Improved Shock Factor to Evaluate the Shock Environment of Small-Sized Structures Subjected to Underwater Explosion," *Shock and Vibration*, Vol 2015, 2015, ID. 451583.

[10] Yuan, Y., and Tan, P. J., "Deformation and failure of rectangular plates subjected to impulsive loadings," *International Journal of Impact Engineering*, Vol. 59, 2013, pp. 46-59.

[11] Desphande, V. S., Heaver, A., and Fleck, N. A., "An underwater shock simulator," *Proceedings of the Royal Society A: Mathematical, Physical and Engineering Science*, Vol. 462, No. 2067, pp. 1021-1041.

[12] Sinclair, J., and Cui, X., "A theoretical approximation of the shock standoff distance for supersonic flows around a circular cylinder," *Physics of Fluids*, Vol. 29, No. 2, 2017, pp. 026102.1-026102.13.

[13] Rajendran, R., and Lee, J. M., "Blast loaded plates," *Marine Structures*, Vol. 22, No. 2, 2009, pp. 99-127.